

# Shape and Buckling Transitions in Solid-Stabilized Drops<sup>†</sup>

Hui Xu,<sup>‡</sup> Sonia Melle,<sup>§</sup> Konstantin Golemanov,<sup>‡</sup> and Gerald Fuller<sup>\*,‡</sup>

Department of Chemical Engineering, Stanford University, Stanford, California,  
 Departamento de Óptica, Facultad de Ciencias Físicas, Universidad Complutense de Madrid,  
 Ciudad Universitaria, 28040 Madrid, Spain, and Laboratory of Chemical Physics and  
 Engineering, Faculty of Chemistry, University of Sofia, 1164 Sofia, Bulgaria

Received March 20, 2005. In Final Form: June 13, 2005

We study shape and buckling transitions of particle-laden sessile and pendant droplets that are forced to shrink in size. Monodisperse polystyrene particles were placed at the interface between water and decane at conditions that are known to produce hexagonal, crystalline arrangements on flat interfaces. As the volumes of the drops are reduced, the surface areas are likewise diminished. This effectively compresses the particle monolayer coating and induces a transition from a fluid film to a solid film. Since the particles are firmly attached to the interface by capillary forces, the shape transitions are reversible and shape/volume curves are the same for drainage and inflation. Measurements of the internal pressure of the drops reveal a strong transition in this variable as the buckling transition is approached.

## Introduction

The study of colloidal particles adsorbed at a liquid–liquid interface is very important for fundamental and technological reasons. The behavior of colloidal particles confined to the interface between two different liquid phases is of particular interest as they serve as a model system to study crystallization processes<sup>1,2</sup> and is also significant in industrial applications such as the stabilization of so-called Pickering emulsions.<sup>3–5</sup> Important processes that occur with emulsions are desiccation<sup>6</sup> and Ostwald ripening.<sup>7</sup> In either case, droplets are reduced in volume and surface-active materials can become compressed at the interface. The former process can occur with either drops attached to surfaces in the form of pendant or sessile drops or suspended in air, as in the case of spray drying. The majority of previous studies on the collapse of droplets have considered the problem of desiccation<sup>6,8–10</sup> and have reported on remarkable shape transitions by evaporating droplets composed of complex liquids consisting of polymer solutions or particulate

suspensions. Recently, Asekomhe et al.<sup>11</sup> have reported on the buckling of pendant water droplets coated with particles and surrounded by oil. A droplet of liquid encapsulated by a “clean” interface that is only characterized by a surface tension will be reduced in size in a manner that is completely described by the Young–Laplace equation. In the absence of gravity, a suspended droplet will remain spherical and the internal pressure will increase in inverse proportion to the decreasing drop radius. If the droplet is sessile, it will shrink as a spherical cap and its contact angle will remain constant. The situation is completely changed if the droplet interface becomes laden with particles. This can induce a transition from an interface that is fluid and only characterized by a surface tension toward a solid film that possesses elastic moduli and that can sustain anisotropic stresses.

The transition from a fluid film to a solid film is manifested in shape transitions and buckling of droplets as their volumes are decreased. This phenomenon has recently been analyzed for the case of “rafts” of noncolloidal particles floating at the air/water interface between barriers that can compress them.<sup>12</sup> Ultimately, the particles are compressed together to the point that the layer buckles and forms an undulating surface with a characteristic wavelength. This is quite a general pattern and had been observed previously for colloidal particles by Aveyard and co-workers.<sup>13</sup> Mahadevan and co-workers<sup>12</sup> have developed a simple mechanical model for such rafts that predicts that the Young’s modulus,  $E$ , depends on the surface tension,  $\gamma$ , and particle diameter,  $d$ , as  $E = 4.54\gamma/d$ . This assumes a contact angle of 90° and perfectly spherical, hard spheres that are close-packed in a hexagonal arrangement. Furthermore, by modeling this problem as analogous to the buckling of an elastic beam, the wavelength of the undulations can be directly related to the Young’s modulus. Using these results, they developed a “buckling” assay where measurement of the

<sup>†</sup> Part of the Bob Rowell Festschrift Special Issue.

<sup>\*</sup> To whom correspondence should be addressed.

<sup>‡</sup> Stanford University.

<sup>§</sup> Universidad Complutense de Madrid.

<sup>‡</sup> University of Sofia.

(1) Pieranski, P. Two-dimensional interfacial colloidal crystals. *Phys. Rev. Lett.* **1980**, *45*, 569–572.

(2) Aveyard, R.; et al. Measurement of Long-Range Repulsive Forces between Charged Particles at an Oil–Water Interface. *Phys. Rev. Lett.* **2002**, *88*, 246102.

(3) Pickering, S. U. Emulsions. *J. Chem. Soc.* **1907**, *91*, 2001–2021.

(4) Aveyard, R.; Binks, B. P.; Clint, J. H. Emulsions stabilised solely by colloidal particles. *Adv. Colloid Interface Sci.* **2003**, *100*, 503–546.

(5) Melle, S.; Lask, M.; Fuller, G. G. Pickering emulsions with controllable stability. *Langmuir* **2005**, *21*, 2158–2162.

(6) Pauchard, L.; Parisse, F.; Allain, C. Influence of salt content on crack patterns formed through colloidal suspension desiccation. *Phys. Rev. E* **1999**, *59*, 3737–3740.

(7) Adamson, A. W.; Gast, A. P. *Physical Chemistry of Surfaces*, 6th ed.; Wiley: New York, 1997.

(8) Tsapis, N.; Dufresne, E. R.; Sinha, S. S.; Riera, C. S.; Hutchinson, J. W.; Mahadevan, L.; Weitz, D. A. Onset of buckling in drying droplets of colloidal suspensions. *Phys. Rev. Lett.* **2005**, *94*, 018302.

(9) Gorand, Y.; Pauchard, L.; Calligari, G.; Hullin, J. P.; Allain, C. Mechanical Instability Induced by the Desiccation of Sessile Drops. *Langmuir* **2004**, *20*, 5138–5140.

(10) Pauchard, L.; Allain, C. Buckling instability induced by polymer solution drying. *Europhys. Lett.* **2003**, *62*, 897–903.

(11) Asekomhe, S. O.; Chiang, R.; Masliyah, J. H.; Elliott, J. A. W. Some Observations on the Contraction Behavior of a Water-in-Oil Drop with Attached Solids. *Ind. Eng. Chem. Res.* **2005**, *44*, 1241–1249.

(12) Vella, D.; Aussillous, P.; Mahadevan, L. Elasticity of an interfacial particle raft. *Europhys. Lett.* **2004**, *68*, 212–218.

(13) Aveyard, R.; Clint, J. H.; Nees, D.; Pauno, V. N. Compression and structure of monolayers of charged latex particles at air/water and octane/water interfaces. *Langmuir* **2000**, *16*, 1969–1979.

wavelength of wrinkling instabilities can be used to estimate the Young's modulus and thereby test microstructural theories for this property. Indeed, they were able to obtain quantitative agreement between the predictions of the model and a series of experiments involving a wide range of particle types and sizes. In the present paper, we experimentally study the shrinkage of droplets where only the interface is laden with particles in contrast to previous studies that have considered the desiccation of suspensions with particles distributed throughout the volume. We also offer measurements of the internal droplet pressure during the process of contraction and expansion.

### Experimental Section

We study the dynamical draining process of both sessile and pendant drops. Both water drops surrounded by decane and the inverse configuration of decane drops immersed in water are studied. The water is composed of a 10 mM NaCl aqueous solution for the case of sessile drops and 100 mM NaCl aqueous solution for pendant drops. The decane (purchased from Fisher at 99.9% purity) is first passed three times through a column of aluminum oxide (Fisher) to remove any polar contaminants that may have been present.

The spherical polystyrene (PS) particles are purchased from Interfacial Dynamics Corporation. They have diameters of 3.1  $\mu\text{m}$ , surface charge density of 9.1  $\mu\text{C}/\text{cm}^2$ , and monodispersity of  $\text{CV} = 3\%$ . First, the particles are dispersed in a 20% isopropyl alcohol solution (from Mallinckrodt) to facilitate their spreading at the decane–water interface. The concentration of particles in the isopropyl alcohol solution is  $5 \times 10^8$  particles/mL. Once the drops are attached to either a flat substrate in the case of sessile drops or to an orifice in the case of pendant drops, we inject a certain volume of the PS particles solution onto the decane–water interface. Then, the system is allowed to come to equilibrium so that the PS particles uniformly covered the drop surface. These particles are preferentially wet by decane as compared to the aqueous solution and achieve a contact angle of  $130^\circ$ .<sup>14</sup>

The experimental setup consists of a container made of clear poly(methyl methacrylate) (PMMA) with a flat base made of either poly(tetrafluoroethylene) (PTFE) or polyoxymethylene (Delrin). At the center of the base, a drain (100  $\mu\text{m}$  diameter) is drilled that ultimately leads to a small syringe. Sessile drops are placed on top of the planar PTFE (or Delrin) surface and immediately over the drain, as well as in equilibrium with the continuous phase. Through the drain, the drop volume can be accurately controlled. The protocol starts by filling the plastic container with the continuous-phase liquid. A syringe pump is used to dispense a drop solution through the drain. Once a drop of the desired volume is established, as well as coated with particles, it is subjected to shrinkage or expansion by evacuation or injection of fluid through the drain. The drop shape is recorded using video microscopy. From image analysis, we measure the contact angle ( $\theta$ ), the drop height ( $z$ ), the radius in contact with the flat surface ( $R_c$ ), and the meridian drop diameter ( $d_m$ ).

The pressure of sessile drops is measured using the principle of equilibration of hydrostatic pressure. The experimental setup is depicted in Figure 1. The drop is connected via a tube to a water reservoir, which acts as a hydrostatic pressure head. If the pressure of the drop and the reservoir are identical, then the volume of the drop should maintain constant, otherwise flow will occur and the drop may either shrink or expand. The drop compression and expansion are accomplished through the computer-controlled syringe pump with adjustable flow rate (0.1–10  $\mu\text{L}/\text{min}$ ). By fixing the volume of the drop at a certain time, the pressure of the drop at that moment can be derived by tuning the height of the reservoir through a step motor (see Figure 1) until the equilibrium of pressure is reached between the drop and the reservoir. The pressure of the drop is defined as  $P_{\text{drop}} = P_0 + \rho_a g h_d + P_L$ , where  $P_0$  is the atmospheric pressure,  $\rho_a g h_d$  is

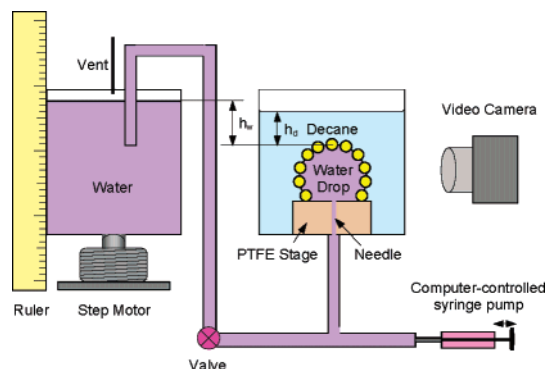


Figure 1. Apparatus to measure the internal droplet pressure.



Figure 2. A sequence of images showing the reduction in the volume of a water droplet within a decane continuum. Note that the droplet shape is nearly spherical.

the hydrostatic pressure due to decane, and  $P_L$  is the Laplace pressure term, which is the object of the measurement. The pressure of the reservoir is simply:  $P_{\text{res}} = P_0 + \rho_w g h_w$ . Equating the two pressures yields  $P_L = (\rho_w h_w - \rho_d h_d)g$ . The densities,  $\rho_w$  and  $\rho_d$ , and the acceleration of gravity,  $g$ , are known parameters, and  $h_d$  can be measured with high precision (see Figure 1). The parameter  $h_w$ , which is variable, can be calibrated using a pure water drop with known interfacial tension with decane (52.3  $\text{mN}/\text{m}$ )<sup>15</sup> and small drop with a constant radius of curvature,  $R$ , so that  $P_L = 2\gamma/R$ . The resolution of this measurement is about  $\pm 1$  Pa, which is small compared to the pressure range encountered in this experiment ( $-10$ – $100$  Pa).

### Results and Discussion

**Uncoated Droplets.** The first set of experiments concern the base case of a “clean” water droplet immersed within decane and subjected to drainage. The case of a sessile drop is shown in Figure 2 where a sequence of images is displayed as the droplet is reduced in size at a constant rate. This situation is completely described by the Young–Laplace equation, and the droplet shapes can be fit to this expression to yield a value for the surface tension. In the experiment shown in Figure 2, the diameter of the drop has been intentionally kept small compared to the capillary length (around 4.5 mm) so that it adopts the shape of a spherical cap. In this case, the internal pressure is simply

$$\Delta P = \frac{2\gamma}{R} \quad (1)$$

where  $R$  is the drop radius. This simple result motivates the plotting of the measured pressure drop as a function of the inverse drop radius, as done in Figure 3. The result is a linear relationship with slope  $2\gamma$ . Indeed, from this slope, we find the surface tension of the water/decane interface to be  $52.1 \pm 1.9$   $\text{mN}/\text{m}$ , which is close to the accepted value of  $52.3 \pm 1.0$   $\text{mN}/\text{m}$ .<sup>15</sup> In this figure, a deviation from a linear relationship is observed for the smallest drop radii, and this is most likely a result of

(14) Stancik, E. J.; Fuller, G. G. Connect the drops: Using solids as adhesives for liquids. *Langmuir* **2004**, *20*, 4805–4808.

(15) Nespolo, S. A.; Chan, D. Y. C.; Grieser, F.; Hartley, P. G.; Stevens, G. W. Forces between a Rigid Probe Particle and a Liquid Interface: Comparison between Experiment and Theory. *Langmuir* **2003**, *19*, 2124–2133.

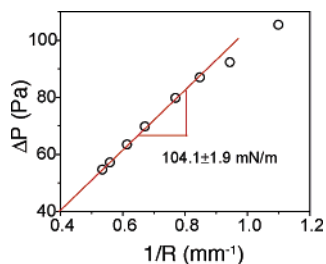


**Figure 3.** The pressure drop across an “uncovered”, sessile droplet of water surrounded by decane plotted as a function of the inverse of the droplet radius.

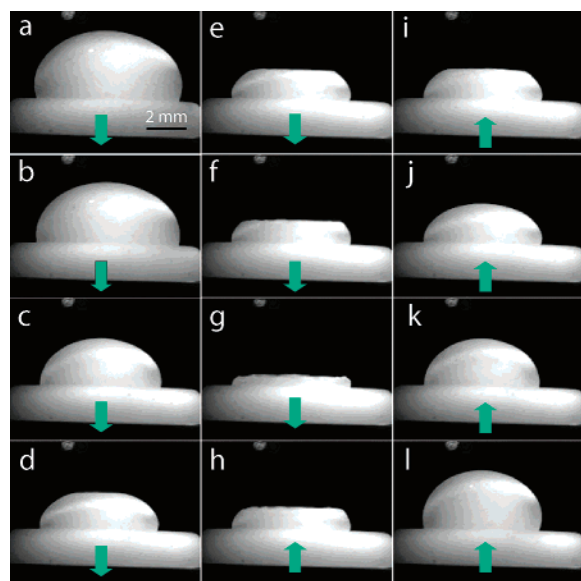


**Figure 4.** The deflation and inflation process of a large PS-covered water drop surrounded by decane. Below each image in the figure is an arrow indicating whether the drop is shrinking (down arrow) or inflating (up arrow).

contamination of the interface by trace amounts of impurities in the bulk liquids.

**Particle-Covered Droplets.** Coating a droplet with particles produces an interface with the potential of undergoing a liquid-to-solid transition as the volume is reduced and the area is likewise diminished. Reducing the available area will compress the particle monolayer and increase the interfacial modulus. However, the energy required to remove a particle of radius  $a$  from an interface with surface tension,  $\gamma$ , is

$$E_{\gamma} = \pi a^2 \gamma (1 \pm \cos \alpha)^2 \quad (2)$$

where  $\alpha$  is the three-phase contact angle.<sup>16</sup> The sign in eq 2 is negative if the particle is removed into the water phase and positive if it is removed to the oil phase. For the  $3 \mu\text{m}$  particles used in this work, this energy is greater than  $10^7$  kT, and this means that the particles are essentially irreversibly attached to the interface.

In Figure 4, a sequence of images showing the deflation and inflation process of a water droplet covered with polystyrene particles and surrounded by decane. Below each image in the figure is an arrow indicating whether the drop is shrinking (down arrow) or inflating (up arrow). Images a–g in Figure 4 show the droplet in various states as the volume is decreased. At some point in the deflation process, the shell starts to collapse (see image d). In

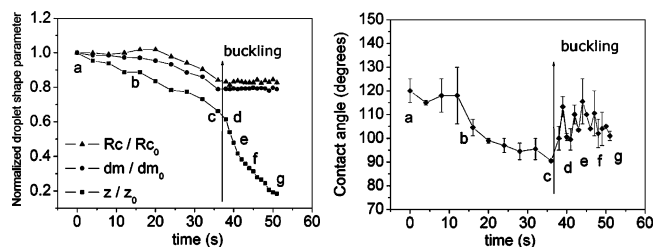


**Figure 5.** Drop shape analysis during the deflation process shown in Figure 4a–g. (Left) Time evolution of contact radius ( $R_c$ ), meridional drop diameter ( $d_m$ ), and drop height ( $z$ ). All variables have been made dimensionless with their initial values. (Right) Time evolution of the contact angle ( $\theta$ ). The letters from a to g correspond to images in Figure 4.

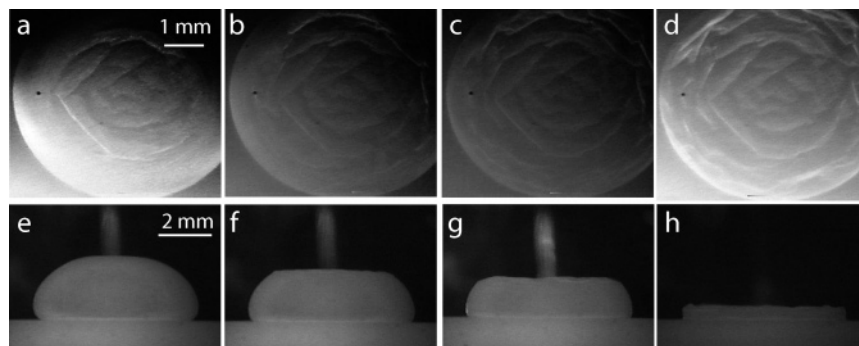
addition, we observe that the droplet can be re-inflated to fully recover its initial shape (see images h–l in Figure 4). A quantitative analysis of the images corresponding to the deflating process is shown in Figure 5. First, after the onset of buckling, the adhesive radius of the droplet,  $R_c$ , remains constant as the height of the droplet,  $z$ , abruptly diminishes (see Figure 5, left). This effect is similar to the case of desiccation of droplets composed of polymer solutions and particle suspensions, and the pinning has been suggested as arising from adsorption of the solutes onto the substrate. Second, because of the pinning of the droplet, the contact angle,  $\theta$ , (as measured from within the droplet) decreases as the droplet is evacuated (see Figure 5, right).

Figure 6 emphasizes the buckling behavior of the rigid shell that forms once the particles jam together. The collapse and buckling of the shell first occurs at the top of the drop, and this is because the Gaussian curvature of the shell is a minimum at that location. This is due to the large size of the drop relative to the capillary length (around 4.5 mm), and this allows gravity to deform its shape away from a spherical cap. The shape instability produces a flattened, circular disk that proceeds downward (see the evolution in drop profiles in Figure 6). Although the internal pressure of this droplet was not measured, the flatness of the top portion indicates that the pressure drop across the interface is near to zero. The morphology of the flattened region is revealed in the top views of Figure 6. A disk is formed with a crumpled topology with undulations that are roughly in the form of concentric, annular ridges. The buckled structures adopted by the system have the minimum Gaussian curvature that can fit into a disk. Similarly to what has been observed on experiments of monolayers of charged latex particles at planar octane–water interfaces under compression,<sup>13</sup> when the drop is being deflated, beyond collapse, the particle monolayer on the drop surface folds and corrugates but there is no expulsion of individual particles or aggregates of particles from the interface.

The onset of buckling instabilities proceeds differently if the droplet is sufficiently small so that its shape is close to that of a spherical cap. Such an experiment is shown in Figure 7. Again, an arrow has been included below each image in the figure indicating whether the drop is shrinking (down arrow) or inflating (up arrow). Note that the buckling is no longer initiated at the top of the drop. Instead, the dimpling occurs at random locations on the drop surface (see image c in the deflation sequence). Indeed, the entire surface of the droplet becomes rough.

The internal pressure of the droplet is shown in Figure 8. Unlike an “unprotected” drop, its internal pressure decreases instead of rising with decreasing volume. There is a large decrease in pressure between the Figure 7b,

(16) Binks, B. P. Particles as surfactants – similarities and differences. *Curr. Opin. Colloid Interface Sci.* **2002**, *7*, 21–41.



**Figure 6.** The deflation process of a PS-covered water drop surrounded by decane. These images were chosen following the onset of buckling. Top view (a–d) and side view (e–h).

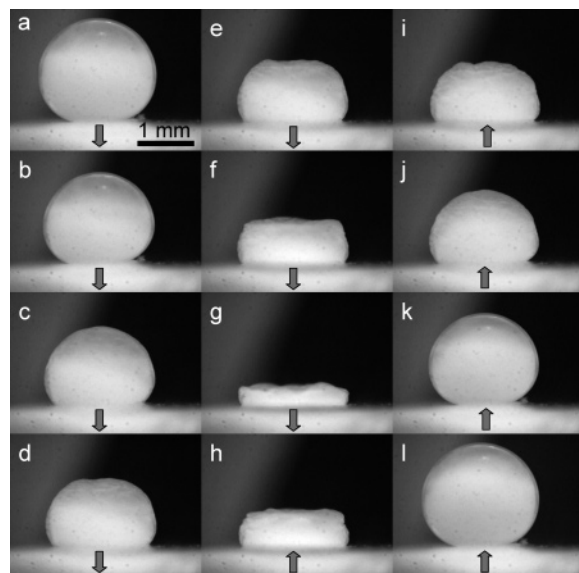


**Figure 7.** The deflation process of a small PS-covered water drop surrounded by decane. The small size of this drop has led to a roughly spherical shape. Below each image in the figure is an arrow indicating whether the drop is shrinking (down arrow) or inflating (up arrow).

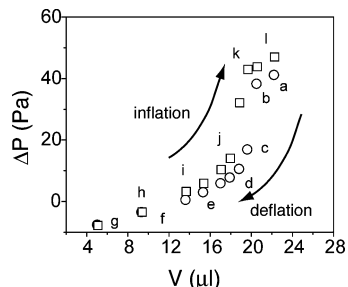


**Figure 8.** The relative, internal pressure of a water droplet coated with polystyrene spheres as a function of its volume during deflation and inflation. The letters from a to l correspond to images in Figure 7.

where there is an absence of dimples, and Figure 7c, where the first dimple appears in that sequence. Upon re-inflation, there is another steep jump in pressure between images j and k that corresponds to the elimination of dimpling. Also note that the pressure–volume curves show a hysteresis between deflation and re-inflation. This is a result of a reconfiguration of the particle microstructure upon compression of the layer, and it requires a finite amount of time for the microstructure to relax following re-inflation.

As noted above, the adhesive area of the shrinking drop remains essentially constant in size once its surface area

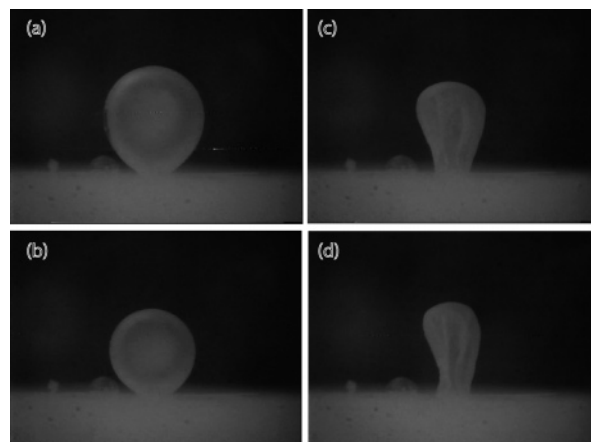


**Figure 9.** The deflation process of a PS-covered decane droplet surrounded by water with 100 mM NaCl. The buoyancy of the decane forces the droplet to be extended upward. This drop was repeatedly inflated/deflated to demonstrate that the particles do not leave the surface.

has been reduced to the point where the particle monolayer is fully compressed. This is evident in Figure 7 where adhesive surface is fixed in size from image c to image j where buckling has occurred. Unlike a droplet with a “clean” interface that reduces its volume with a receding contact perimeter and a constant contact angle, a particle-laden droplet has a pinned contact perimeter and a contact angle that continuously decreases in magnitude as the drop shrinks in size. This sort of behavior has been reported on the desiccation of drops consisting of suspended, colloidal particles.<sup>6</sup> One explanation that has been offered is that the pinning of the contact line is a consequence of adsorbance of the particles against the substrate. The present problem is distinguished from previous studies by the fact that the particles only reside as a monolayer at the interface. If the pinning occurs because of particles adsorbing, it can only occur along the contact line. Another possible explanation is that that perimeter of the contact line consists of a ring of close-packed particles that resist compression and hold the length of the perimeter fixed.

We have also examined the inverse case of an oil (decane) droplet coated with particles and undergoing expansion and compression in the presence of water with 100 mM NaCl. Figure 9 is a sequence of images starting from the original droplet, which is classified as a pendant drop, and chronicles the evacuation of the decane and the buckling of the particle monolayer. As in the case of the sessile water droplets, the interface ultimately crinkles and repeated inflation/deflation cycles indicate that the particles do not leave the interface.

### Conclusions

This work examines the collapse of droplets coated with monolayers of colloidal particles that are pinned to the interface between water and decane. The presence of these particles yield an interface that is ultimately characterized by both a surface energy and surface elasticity. Contraction of the droplet interface upon depletion of its volume ultimately brings the particles into sufficiently close proximity that a liquid film-to-solid film transition occurs. Following this transition, the droplet ultimately behaves much like a rigid shell, and if the pressure difference across the droplet interface becomes too low, buckling ensues. Indeed, direct measurement of this pressure reveals a sharp drop in the pressure upon the onset of dimpling. However, the instability of these shells occurs when the pressure is still positive, unlike a perfectly rigid, thin shell, where a negative pressure drop (a vacuum) would be necessary to achieve this effect. We believe that this is

because a surface energy acts in concert with the surface elasticity. We are presently exploring the possibility of using these pressure measurements combined with analysis of the shape of the drops to extract these properties.

The connection of the interfacial elastic modulus to the microstructure will require a knowledge of the interparticle forces within the monolayer, unlike the treatment followed in ref 12. The systems addressed in that work are noncolloidal, hard spheres, and the model used to predict the Young's modulus is based on calculating the incremental surface energy upon deformation of the microstructural arrangement of the particles.

**Acknowledgment.** The authors acknowledge support from the National Science Foundation and from Unilever Company.

LA0507378